

# Ancestral morphology of crown-group molluscs revealed by a new Ordovician stem aculiferan

Jakob Vinther<sup>1,2\*</sup>, Luke Parry<sup>1,3\*</sup>, Derek E. G. Briggs<sup>4,5</sup> & Peter Van Roy<sup>4,6</sup>

Exceptionally preserved fossils provide crucial insights into extinct body plans and organismal evolution<sup>1</sup>. Molluscs, one of the most disparate animal phyla, radiated rapidly during the early Cambrian period (approximately 535–520 million years ago (Ma))<sup>2</sup>. The problematic fossil taxa *Halkieria*<sup>3</sup> and *Orthrozanclus*<sup>4</sup> (grouped in Sachitida) have been assigned variously to stem-group annelids, brachiopods<sup>4,5</sup>, stem-group molluscs<sup>4</sup> or stem-group aculiferans (Polyplacophora and Aplacophora)<sup>6</sup>, but their affinities have remained controversial owing to a lack of preserved diagnostic characters. Here we describe a new early sachitid, *Calvapilosa kroegeri* gen. et sp. nov. from the Fezouata biota of Morocco<sup>7,8</sup> (Early Ordovician epoch, around 478 Ma). The new taxon is characterized by the presence of a single large anterior shell plate and polystichous radula bearing a median tooth and several lateral and uncinal teeth in more than 125 rows. Its flattened body is covered by hollow spinose sclerites, and a smooth, ventral girdle flanks an extensive mantle cavity. Phylogenetic analyses resolve *C. kroegeri* as a stem-group aculiferan together with other single-plated forms such as *Maikhanella* (*Siphogonuchites*) and *Orthrozanclus*; *Halkieria* is recovered closer to the aculiferan crown. These genera document the stepwise evolution of the aculiferan body plan from forms with a single, almost conchiferan-like shell through two-plated taxa such as *Halkieria*, to the eight-plated crown-group aculiferans. *C. kroegeri* therefore provides key evidence concerning the long debate about the crown molluscan affinities of sachitids. This new discovery strongly suggests that the possession of only a single calcareous shell plate and the presence of unmineralised sclerites are plesiomorphic (an ancestral trait) for the molluscan crown.

Mollusca Linnaeus, 1758

Sachitida He, 1980

(This clade includes Aculifera plus the stem taxa Halkieriidae, *Orthrozanclus*, Siphogonuchitidae)

Siphogonuchitidae Qian, 1977

(This clade contains *Calvapilosa*, *Siphogonuchites*, *Dabashanites*, *Drepanochites*, *Lomasulcachites*, *Lopochites* and *Quadrosiphogonuchites*)

*Calvapilosa kroegeri* gen. et sp. nov.

LSID. urn:lsid:zoobank.org:pub:C0C05357-69A2-4937-A28F-C52854CF2870

**Etymology.** The generic name derives from the Latin *calva*, scalp and *pilosus*, hairy/shaggy for the head plate covered by densely spiculated mantle. Species named after Björn Kröger for ‘discovering’ the holotype in the collections at Yale.

**Holotype.** Yale Peabody Museum (YPM) 237255 (Fig. 1 and Extended Data Figs 1, 3c, 5f–i).

**Referred material.** Paratypes: YPM 227515 (Fig. 2a–c, h, j and Extended Data Figs 2, 3b), YPM 530835 (Extended Data Fig. 4e, f),

YPM 530836 (Fig. 2d–f and Extended Data Figs 3d–e, 4c, d, 5a–e) and YPM 530837 (Extended Data Figs 3a, 4a, b).

Other specimens: ?YPM 227641 (Extended Data Fig. 4g, h), YPM 515766.

**Locality and horizon.** *Calvapilosa* can be found throughout the classical collecting area of the Fezouata biota to the north of Zagora. The holotype was collected in the Bou Zorgan area. The other specimens were found at additional excavations in this area, near Bni Zoli, in the Bou Glf and Tamagrout areas and on the western flank of Jbel Tigzigzaouine. All localities belong to the Fezouata Formation, *Araneograptus murrayi* graptolite biozone, upper Tremadocian stage (Lower Ordovician series). Detailed locality data are curated with the specimens.

**Diagnosis for genus and species.** Elongate sachitid bearing a single, large subquadratic anterior shell plate with an anteriorly placed mucro.

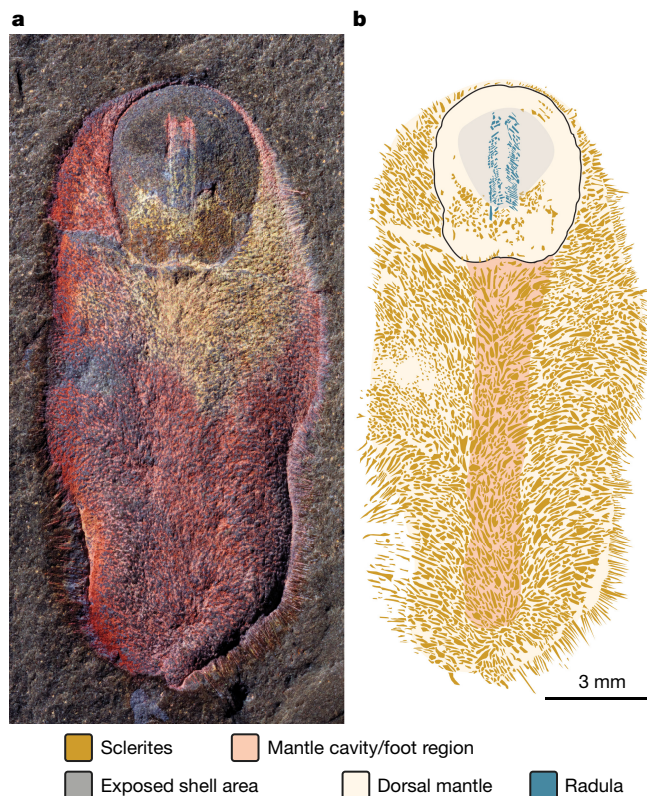


**Figure 1** | *Calvapilosa kroegeri*, holotype YPM 237255, from the Lower Ordovician epoch (Tremadocian age) Fezouata formation, near Zagora, Morocco. **a**, Part, imaged and illuminated from north west. **b**, Interpretative drawing.

<sup>1</sup>School of Biological Sciences, University of Bristol, Life Sciences, Building, 24 Tyndall Avenue, Bristol BS8 1TQ, UK. <sup>2</sup>School of Earth Sciences, University of Bristol, Wills Memorial Building, Queen's Road, Bristol BS8 1RJ, UK. <sup>3</sup>Department of Earth Sciences, The Natural History Museum, Cromwell Road, London SW7 5BD, UK. <sup>4</sup>Department of Geology and Geophysics, Yale University, 210 Whitney Avenue, New Haven, Connecticut 06511, USA. <sup>5</sup>Yale Peabody Museum of Natural History, 170 Whitney Avenue, New Haven, Connecticut 06520, USA. <sup>6</sup>Department of Geology and Soil Science, Ghent University, Krijgslaan 281/S8, B-9000 Ghent, Belgium.

\*These authors contributed equally to this work.

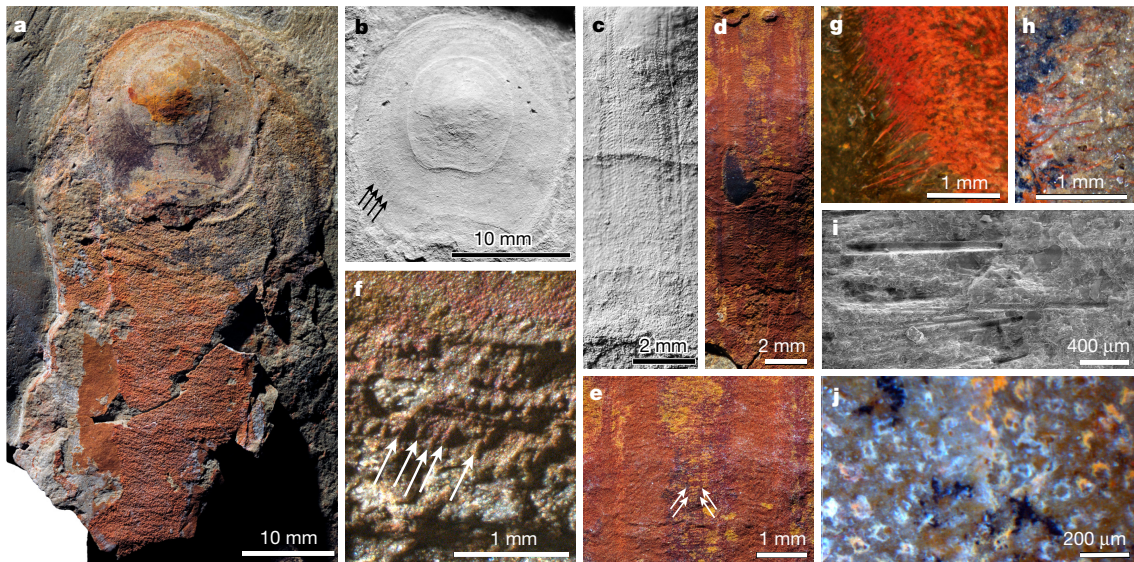


**Figure 2 | Details and additional specimens of *C. kroegeri*.** **a**, Paratype YPM 227515. Part, preserving both the dorsal and ventral mantle (see Extended Data Fig. 3) in addition to the anterior shell. **b**, Radial imprints of putative aesthete canals (arrows). **c**, Radula. **d**, Radula in YPM 530836 (see Extended Data Figs 4, 5). **e**, Detail of **d**, note the attachment base of the median teeth (arrows). **f**, Infilled putative

radial aesthete canals (arrows) of YPM 530836. **g**, Sclerites near margin of YPM 237255 (see Fig. 1). **h**, Sclerites from the folded section of the dorsal mantle of YPM 227515 (**a** and Extended Data Fig. 2). **i**, Secondary electron microscopy (SEM) detail of sclerites in a longitudinal section of YPM 237255. **j**, Sclerites in a cross section of YPM 227515, showing angular external outlines.

Dense dorsal covering of fine, hollow, spinose sclerites with inconspicuous morphological zonation. Shell plate largely covered by the mantle and sclerites (Fig. 3 and Extended Data Fig. 6).

The single anterior shell plate is subquadratic in outline, the apex (mucro) situated anterior of the mid-length resulting in a steeper anterior than posterior slope (Fig. 2a, b and Extended Data Fig. 4). A shallow concave posterior median indentation in the shell plate of smaller (subadult or juvenile) individuals (Fig. 1) is subdued into an almost straight margin in larger specimens (Extended Data Fig. 4). The shell plate exhibits holoperipheral growth. Partially infilled structures along the margin may be aesthete canals<sup>6</sup> (Fig. 2a, b, f). The dorsal surface of the mantle is covered with hollow spinose sclerites, which do not appear to be arranged in distinct morphological zones. If sclerites are present on the ventral surface they are too small to be discerned ( $<40\mu\text{m}$ ). The ventral mantle is preserved as a smooth brown-stained surface (Fig. 2a and Extended Data Figs 2a–d, 5, 7). The mantle cavity (evident as a ridge in YPM 227515 and a colour difference in YPM 237255) extends along the entire length of the trunk. The radula bears at least 125 tooth rows comprising a median tooth and several flanking teeth (Fig. 2c–e and Extended Data Figs 3, 5a–e). These can be divided into lateral and uncinal teeth using terminology applicable to chitons<sup>9</sup> (Extended Data Figs 3e, 5a–e), but the exact number is difficult to discern. The median tooth is separated from a major cusp by at least four smaller lateral teeth (Extended Data Figs 3e, 5d). A suite of oblique and posteriorly oriented uncinal teeth lies further abaxially (Extended Data Figs 3e, 5b, c, e).

The position of the radula confirms that the shell plate is anterior. A posterior shell plate, such as that in *Halkieria evangelista*<sup>3,5</sup> (and probably also *Oikozetetes*), is absent (Figs 1, 2 and Extended Data Figs 1, 2): the cover of dorsal sclerites is uninterrupted where such a plate would be situated (Fig. 1).

The body of the holotype YPM 237255 (Fig. 1), which is the smallest known specimen, is 16.7 mm long and 7.6 mm wide, whereas the almost complete YPM 227515 (Fig. 2 and Extended Data Fig. 2a, b) is 68.3 mm in preserved length and at least 31 mm wide. Extrapolating from the largest isolated shell plates (Extended Data Fig. 4), individuals reached at least 120 mm in length. Sclerites vary in cross section from polygonal to square to circular (Fig. 2j). The dorsal sclerites in YPM 227515 are  $54\mu\text{m} \pm 20\mu\text{m}$  in diameter internally, approximately  $70\mu\text{m}$  externally,

and about 0.8 mm long (Fig. 2i, j and Extended Data Fig. 2f, g). Those in the holotype may solely be preserved as diagenetic infills (Extended Data Figs 3, 5f–i), and are  $57\mu\text{m} \pm 20\mu\text{m}$  in diameter and vary from 0.5–1.2 mm in length. It therefore appears that the sclerites in the juveniles were larger relative to their body size. An isolated shell

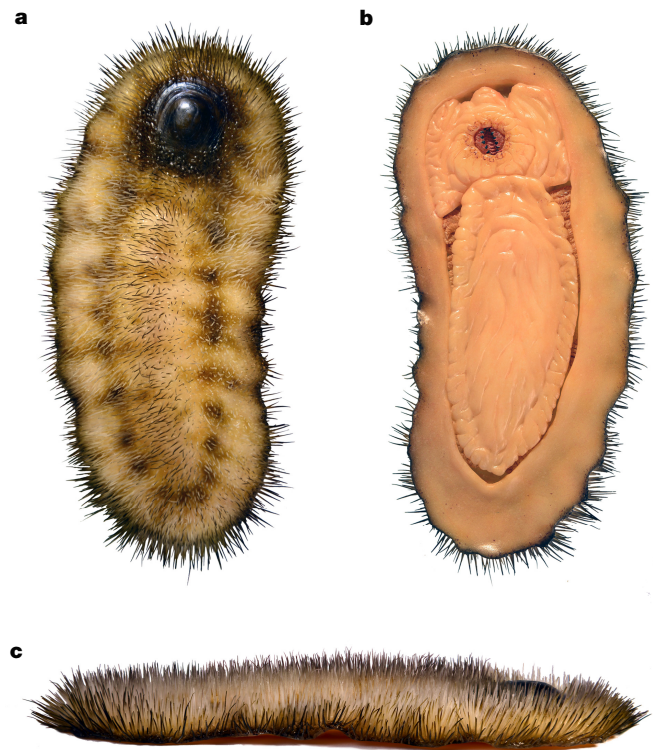


**Figure 3 | Reconstruction of *Calvapilosa kroegeri*, juvenile.** **a**, Dorsal view. **b**, Ventral view. **c**, Lateral view. Colour scheme is speculative, whereas soft tissues are inferred by phylogenetic bracketing. See also Extended Data Fig. 7. Resin model constructed by E. Horn (<http://www.10tons.dk/>).

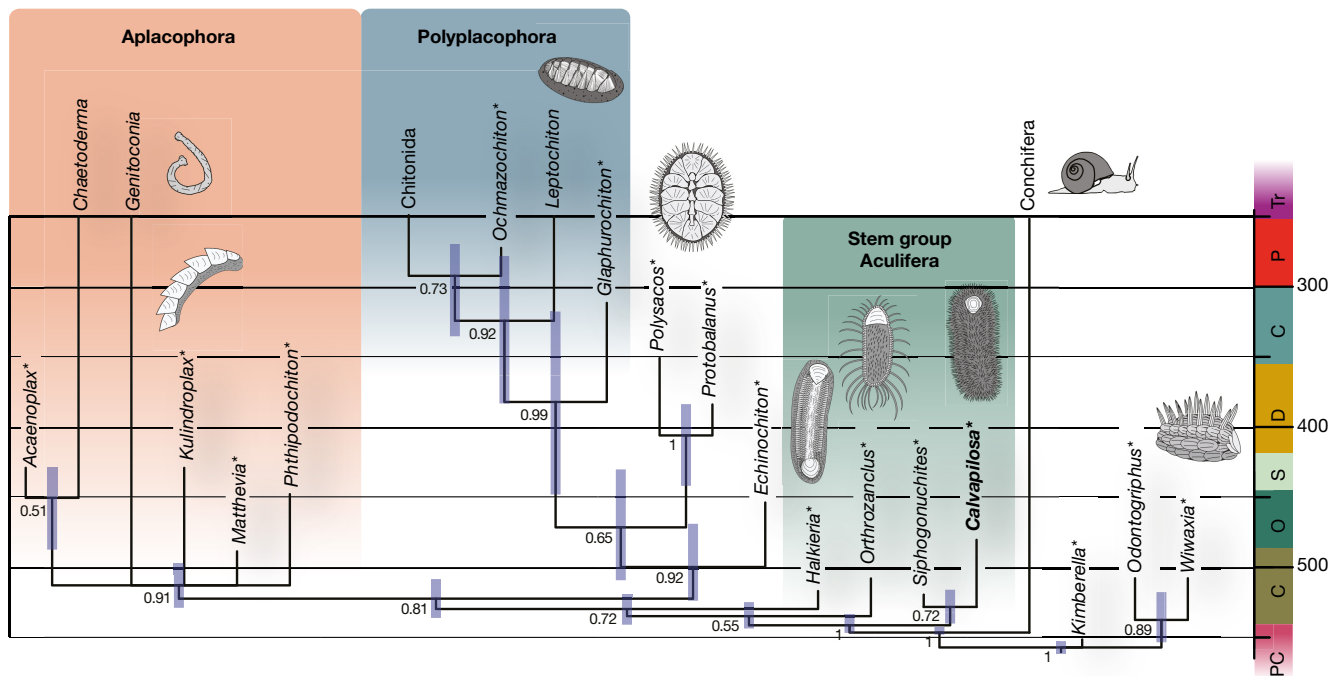


**Figure 4 | Time tree of aculiferan evolution based on a Bayesian total evidence analysis.** Based on 62 taxa, 134 morphological characters and 2,054 amino acid loci analysed in MrBayes. Error bars (purple shading) at the nodes are 95% highest posterior density (HPD) intervals, and the time axis is truncated at the end of the Permian period and within the Ediacaran period. See Extended data Figs 8, 9 and Supplementary

Information for details of the phylogenetic analysis. Commands to run the total evidence analysis are included in the NEXUS file of the Supplementary Information. Scale in millions of years before present. PC, Precambrian time; C, Cambrian period; O, Ordovician period; S, Silurian period; D, Devonian period; C, Carboniferous period; P, Permian period; Tr, Triassic period. Extinct taxa are indicated with an asterisk.

(YPM 227641) plate differs in the details of its shape and is therefore only tentatively assigned to *C. kroegeri* (Extended Data Fig. 4g, h).

The phylogenetic position of sachtitids and wiwaxiids, which have been grouped together into Halwaxiida by some authors<sup>4</sup>, has been a topic of debate. Sachtitids have been interpreted as stem brachiopods<sup>5,10</sup> or basal aculiferan molluscs<sup>6,11</sup>, whereas halwaxiids as a whole have been considered to represent either stem molluscs<sup>4,12</sup>, or the stem group of both brachiopods and annelids<sup>4</sup> (see Supplementary Information). *C. kroegeri* provides new data, which allow the affinities of sachtitids and wiwaxiids to be clarified. It possesses a number of unequivocal molluscan synapomorphies identified here in sachtitids, including a radula and mantle cavity, together with mineralized sclerites and a shell plate. Such a combination occurs only in aculiferan molluscs (chitons and aplacophorans) among extant taxa. *C. kroegeri* is distinguished from other sachtitids by the possession of slender, spinose sclerites and the lack of conspicuous sclerite zones (distinct sclerite zones may also have been absent in siphogonuchitids<sup>13</sup>). Sclerite morphology and zonation also vary among modern aculiferans<sup>9</sup>.

Our phylogenetic analysis (Fig. 4, Extended Data Figs 8, 9, see Supplementary Information and nexus files with character matrices) suggests an evolutionary sequence from Cambrian sachtitids, via *C. kroegeri*, towards crown aculiferans. The analysis indicates that a single anterior shell plate was acquired before the addition of further shell plates in *Halkieria* and crown-group aculiferans. Fossil, morphological and molecular data using a total evidence approach<sup>14</sup> suggest that the aculiferan crown group diversified around the boundary between Cambrian and Ordovician periods<sup>15</sup> (Fig. 4 and Extended Data Fig. 9). The earliest crown or upper-stem aculiferans (for example, *Matthevia*<sup>15</sup>) have an anterior holoperipheral valve followed by seven self-similar mixoperipheral and/or hemiperipheral valves. Extant chitons maintain the plesiomorphic complement of eight shell plates but this number is reduced, ultimately to zero, in aplacophorans. This loss is heralded by the presence of seven shell plates in the Silurian total group aplacophorans *Acaenoplax*<sup>16</sup> and *Kulindroplax*<sup>17</sup>, and

echoed in seven serially repeated calcium-secreting papillae in living *Chaetoderma*<sup>18</sup> and seven iterated regions in a neomeniomorph aplacophoran post-larva<sup>11</sup>. During development, the anterior and intermediate shell plates form first and the posterior shell plate is added later<sup>19</sup>. The absence of a holoperipheral posterior shell plate in *Kulindroplax* may indicate that it was lost before the intermediate and anterior shell plates in aplacophorans, and supports the scenario in which aplacophorans evolved through progenetic pedomorphosis<sup>20</sup>. We recovered the 17-plated multiplacophorans<sup>21</sup> outside the polyplacophoran crown group, in a similar position to that obtained previously<sup>22</sup>. Our analyses therefore suggest that the separation of lateral shell plates in Multiplacophora is a distinctive feature that is not related to the origin of the aculiferan or polyplacophoran body plan. The similarities between multiplacophoran shells and those in crown-group chitons<sup>21,22</sup>, and even in very derived Cretaceous chitons<sup>22</sup>, suggests convergent evolution.

The placement of *C. kroegeri*, *Halkieria* and the other sachtitids on the stem of Aculifera, rather than on the molluscan stem, allows us to generate a new hypothesis for the assembly of the molluscan body plan. The ancestral mollusc was previously considered shell-less and aplacophoran-like<sup>23</sup> or showing the eightfold serialization evident in chitons and the soft tissues of monoplacophorans<sup>24</sup>. Evidence from molecules, fossils and morphology, however, indicates that the aculiferan morphology is not plesiomorphic—the group is a derived clade and sister taxon to conchiferans<sup>25</sup>. Aplacophorans lost their shells secondarily—therefore the characteristics shared by polyplacophorans and conchiferans, such as the possession of a shell, are plesiomorphic for the molluscan crown group.

The presence of multiple muscle scars in monoplacophorans, fossil cephalopods<sup>26</sup> and bivalves has been used as evidence of a chiton-like ancestor for conchiferans. The phylogenetic position of *C. kroegeri*, however, indicates that a single shell is a synapomorphy of Aculifera as well as Conchifera. This is consistent with the fossil evidence: diverse conchiferans and sachtitids appear in the earliest Cambrian

(around 535 Ma) whereas the first unequivocal multivalved chiton-like fossils are late Cambrian in age (around 495 Ma)<sup>27</sup>. Therefore, the evidence suggests that a single shell was present in the molluscan crown ancestor.

Analysis of *C. kroegeri* suggests that the ancestral radula comprised a median tooth and several lateral teeth, the heterodontous and polystichous condition found in chitons and several living conchiferans. Comparable morphologies are found in *Odontogriphus* and *Wiwaxia*<sup>28</sup> from the Burgess Shale, which we recovered on the molluscan stem (Fig. 4), but the radulae of these taxa are characterized by only 3–4 largely undifferentiated tooth rows. The radula was lost in bivalves and reduced in some aplacophorans such as *Chaetoderma*, which has a single tooth row<sup>29</sup>.

Aculiferan sclerites are chitinous structures enveloping a calcareous body<sup>6</sup>. The chitinous bristles of chitons and juvenile octopods are probably homologous, and probably represent a synapomorphy of a spiralian subgroup<sup>30</sup>. Unmineralised chitinous sclerites are also present in wiwaxiids, suggesting that they were also a feature of the ancestral mollusc.

The discovery of a well-preserved radula in an articulated sachtid demonstrates their molluscan affinities and provides a probable answer to the phylogenetic position of these animals. The morphology of *C. kroegeri* provides key evidence informing the stepwise evolution of the aculiferan body plan from a single shelled form, via two shells, to the eight-plated chitons and secondarily reduced vermiform aplacophorans. Our new discovery suggests that the last common ancestor of aculiferans and conchiferans possessed a radula with numerous rows of differentiated teeth, non-biomineralised chaetae and a single calcareous shell. This body plan gave rise to the remarkable morphological diversity characteristic of the molluscan classes—a disparity that has confounded previous attempts to reconstruct the evolutionary history of the group.

**Online Content** Methods, along with any additional Extended Data display items and Source Data, are available in the online version of the paper; references unique to these sections appear only in the online paper.

Received 2 October; accepted 13 December 2016.

Published online 6 February 2017.

- Briggs, D. E. G. Extraordinary fossils. *Am. Sci.* **79**, 130–141 (1991).
- Vinther, J. The origins of molluscs. *Palaeontology* **58**, 19–34 (2015).
- Conway Morris, S. & Peel, J. S. Articulated halkieriids from the Lower Cambrian of north Greenland. *Nature* **345**, 802–805 (1990).
- Morris, S. C. & Caron, J.-B. Halwaxiids and the early evolution of the lophotrochozoans. *Science* **315**, 1255–1258 (2007).
- Conway Morris, S. & Peel, J. S. Articulated halkieriids from the Lower Cambrian of north Greenland and their role in early protostome evolution. *Phil. Trans. R. Soc. Lond. B* **347**, 305–358 (1995).
- Vinther, J. The canal system in sclerites of Lower Cambrian *Sinosachites* (Halkieriidae: Sachtitida): significance for the molluscan affinities of the sachtitids. *Palaeontology* **52**, 689–712 (2009).
- Van Roy, P. et al. Ordovician faunas of Burgess Shale type. *Nature* **465**, 215–218 (2010).
- Van Roy, P., Briggs, D. E. G. & Gaines, R. R. The Fezouata fossils of Morocco: an extraordinary record of marine life in the Early Ordovician. *J. Geol. Soc. Lond.* **172**, 541–549 (2015).
- Schwabe, E. Illustrated summary of chiton terminology. *Spixiana* **33**, 171–194 (2010).
- Williams, A. & Holmer, L. E. Shell structure and inferred growth, functions and affinities of the sclerites of the problematic *Micrina*. *Palaeontology* **45**, 845–873 (2002).
- Scheltema, A. H. & Ivanov, D. L. An aplacophoran postlarva with iterated dorsal groups of spicules and skeletal similarities to Paleozoic fossils. *Invertebr. Biol.* **121**, 1–10 (2002).
- Sigwart, J. D. & Sutton, M. D. Deep molluscan phylogeny: synthesis of palaeontological and neontological data. *Proc. R. Soc. B* **274**, 2413–2419 (2007).
- Bengtson, S. The cap-shaped Cambrian fossil *Maikhanella* and the relationship between coeloscleritophorans and molluscs. *Lethaia* **25**, 401–420 (1992).
- Ronquist, F. et al. A total-evidence approach to dating with fossils, applied to the early radiation of the hymenoptera. *Syst. Biol.* **61**, 973–999 (2012).
- Vinther, J., Sperling, E. A., Briggs, D. E. G. & Peterson, K. J. A molecular palaeobiological hypothesis for the origin of aplacophoran molluscs and their derivation from chiton-like ancestors. *Proc. R. Soc. B* **279**, 1259–1268 (2012).
- Sutton, M. D., Briggs, D. E. G., Siveter, D. J. & Siveter, D. J. An exceptionally preserved vermiform mollusc from the Silurian of England. *Nature* **410**, 461–463 (2001).
- Sutton, M. D., Briggs, D. E. G., Siveter, D. J., Siveter, D. J. & Sigwart, J. D. A Silurian armoured aplacophoran and implications for molluscan phylogeny. *Nature* **490**, 94–97 (2012).
- Nielsen, C., Haszprunar, G., Ruthensteiner, B. & Wanninger, A. Early development of the aplacophoran mollusc *Chaetoderma*. *Acta Zool.* **88**, 231–247 (2007).
- Eernisse, D. J. & Reynolds, P. D. in *Microscopic Anatomy of the Invertebrates* Vol. 5 (eds Harrison, F. W. & Kohn, A. J.) 55–110 (Wiley-Liss, 1994).
- Scheltema, A. H. Aplacophora as progenetic aculiferans and the coelomate origin of mollusks as the sister taxon of Sipuncula. *Biol. Bull.* **184**, 57–78 (1993).
- Vendrasco, M. J., Wood, T. E. & Runnegar, B. N. Articulated Palaeozoic fossil with 17 plates greatly expands disparity of early chitons. *Nature* **429**, 288–291 (2004).
- Vinther, J. et al. The origin of multiplacophorans—convergent evolution in aculiferan molluscs. *Palaeontology* **55**, 1007–1019 (2012).
- Salvini-Plawen, L. & Steiner, G. in *Origin and Evolutionary Radiation of the Mollusca* (ed. Taylor, J. D.) 29–51 (Oxford Univ. Press, 1996).
- Wingstrand, K. G. On the anatomy and relationships of recent Monoplacophora. *Galathea Reports* **16**, 7–94 (1985).
- Smith, S. A. et al. Resolving the evolutionary relationships of molluscs with phylogenomic tools. *Nature* **480**, 364–367 (2011).
- Kröger, B. & Mutvei, H. Nautiloids with multiple paired muscle scars from Lower–Middle Ordovician of Baltoscandinavia. *Palaeontology* **48**, 781–791 (2005).
- Vendrasco, M. J. & Runnegar, B. Late Cambrian and Early Ordovician stem group chitons (Mollusca: Polyplacophora) from Utah and Missouri. *J. Paleontol.* **78**, 675–689 (2004).
- Smith, M. R. Mouthparts of the Burgess Shale fossils *Odontogriphus* and *Wiwaxia*: implications for the ancestral molluscan radula. *Proc. R. Soc. B* **279**, 4287–4295 (2012).
- Scheltema, A. H. The radula of the chaetodermatidae (Mollusca, Aplacophora). *Z. Morph. Tiere* **72**, 361–370 (1972).
- Schiemann, S. M. et al. Clustered brachiopod Hox genes are not expressed collinearly and are associated with lophotrochozoan novelties. Preprint at <http://dx.doi.org/10.1101/058669> (2016).

**Supplementary Information** is available in the online version of the paper.

**Acknowledgements** M., B. and L. ‘Ou Said’ Ben Moula collected the specimens and provided support in the field. B. Kröger ‘discovered’ the holotype in 2014 among freshly collected and, at the time uninventoried, material at the YPM. L. Ben Moula and B. Tahiri provided practical assistance. S. Butts and J. Utrup curated specimens and facilitated access to the collections at the YPM. C. Graham provided support and access to digital imaging facilities at the Yale Digital Collections Center (YDC2). The drawings of *C. kroegeri* were made by Z. Dutta and the physical reconstruction was done by E. Horn (<http://www.10tons.dk/>). The research was supported by National Science Foundation Grant EAR-1053247 and by the Division of Invertebrate Paleontology, YPM.

**Author Contributions** J.V. initially analysed the fossils and wrote the first manuscript draft with substantial input to both from all other authors. L.P. and J.V. assembled the character matrix. L.P. did the phylogenetic analyses and produced the interpretative drawings. P.V.R., J.V. and L.P. photographed the fossils. P.V.R. obtained the specimens and locality information through M. ‘Ou Said’ Ben Moula, and prepared the fossils. D.E.G.B. facilitated curation and accession of material to YPM.

**Author Information** Reprints and permissions information is available at [www.nature.com/reprints](http://www.nature.com/reprints). The authors declare no competing financial interests. Readers are welcome to comment on the online version of the paper. Correspondence and requests for materials should be addressed to J.V. ([jakob.vinther@bristol.ac.uk](mailto:jakob.vinther@bristol.ac.uk)).

**Reviewer Information** *Nature* thanks S. Bengtson and the other anonymous reviewer(s) for their contribution to the peer review of this work.

## METHODS

No statistical methods were used to predetermine sample size.

The fossils were mechanically prepared using PaleoToolsME9100, PaleoAro, MicroJack5 and MicroJack1 air scribes, and needles and scalpels. Specimens were glued with Paraloid B-72 dissolved in acetone.

Lighting for the overview photographs of dry, uncoated specimens was provided by a Schott KL 1500 fibre-optic light source with moveable polarizers fitted at the end of the goosenecks; a Cokin XPro X164 circular polarizer was mounted on the camera lens and crossed with the polarizer of the light source to maximize contrast. All parts were lit from the northwest. Counterparts were illuminated from the southwest and mirrored horizontally in Adobe Photoshop CC 2015.4 to create a false-positive relief image and facilitate direct comparison of part and counterpart. Photographs were taken with a Hasselblad H4D-200MS medium-frame digital single-lens reflex camera attached to a computer and operated remotely in six-shot mode through Hasselblad Phocus 8.2.1 software to acquire images of 200-megapixel resolution using a Hasselblad HC Macro 4/120 mm II lens stopped down to  $f/9.5$ . Lens distortion was corrected using Hasselblad Phocus 8.2.1 software. Stacks of between 20 and 50 images were taken in aperture priority mode, with manual focusing through the focal plane. After exporting the FFF-format digital negatives to TIFF from Hasselblad Phocus 8.2.1, the photographs were stacked in Zerene Stacker Pro 1.04 Build T201602151850 (64 bit) using the PMax pyramid stack algorithm. The stacked images were then post-processed in Adobe Photoshop CC 2015.4, first applying the sharpen function, followed by removal of the background. Levels were then manually balanced while holding down the 'alt' key to prevent clipping of pixels in the specimen; the grey level was always retained at 50%. In a few cases, some minor adjustments were made to the exposure. The high-resolution images were down-sampled in Adobe Photoshop CC 2015.4 to lower resolution TIFF files for use in the plates.

Additional photographs were taken with a Nikon d800 using a 105 mm microNikkor lens with or without a  $2\times$  teleconverter. Images were taken using a variety of configurations and lighting conditions, including crossed polarized light and normal incident light, in order to highlight different features. Details were imaged under a Leica M60 or M205 C microscope. In some cases, specimens were whitened with ammonium chloride before photography to enhance contrast.

Specimens were also imaged in a Zeiss Sigma HD VP Field Emission SEM to reveal fine details and preservation of shell plates and sclerites. Specimens were imaged uncoated using both backscatter and secondary electron imaging. Backscatter images were taken at a working distance of 5.5–11.1 mm and secondary electron images were taken at 7.2–8.7 mm.

A morphological matrix of 62 taxa and 134 morphological characters was analysed using equal and implied weights ( $k=3$ ) parsimony with TNT 1.1<sup>31</sup> using traditional search options with 10,000 replicates. Suboptimal trees were saved to generate Bremer support values for equal weights analyses. Jackknife, bootstrap (equal weighting) and symmetric resampling (implied weighting) frequencies were generated using 1,000 replicates.

Bayesian analyses of the morphological data used MrBayes 3.2.6<sup>32</sup> and were performed under the  $mkv + \Gamma$  model for discrete characters for 5,000,000 generations, with 25% burn-in.

Total evidence analyses were performed using a modified version of a published molecular dataset<sup>15</sup> consisting of 2,054 concatenated amino acids from 7 nuclear house-keeping genes with MrBayes 3.2.6 under the uniform tree prior using the IGR clock model, and  $mkv + \Gamma$  and  $LG + I + \Gamma$  for the morphological and

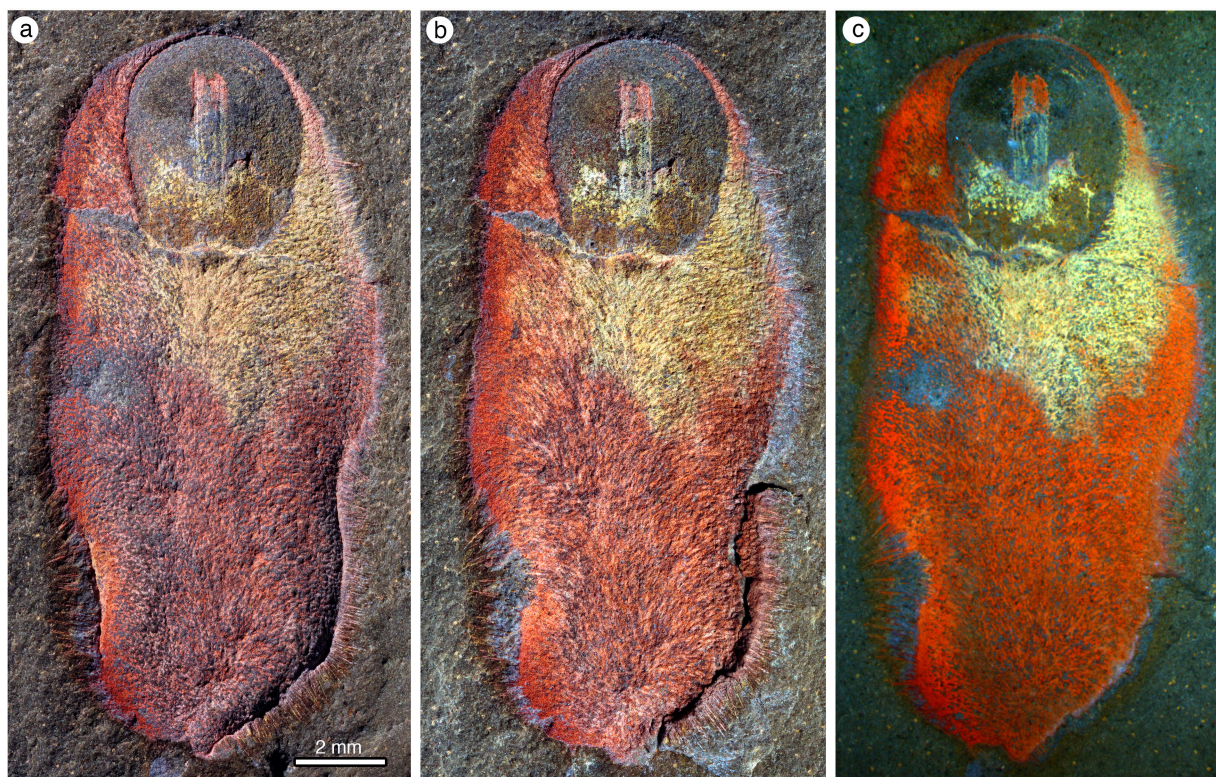
molecular partitions, respectively. Rather than treating fossils as having fixed ages<sup>14</sup>, uncertainties of fossil ages were given by uniform distributions with upper and lower age bounds<sup>33</sup> derived from the Paleobiology Database (PBDB) or the age given in the description of a given taxon. The age of *Kimberella* was established using the generally accepted age of 558–550 Ma for the White Sea assemblage<sup>34,35</sup>. The divergence of *Mytilus* and *Modiolus* was given the same minimum age constraint as in previous analyses<sup>15</sup>, using an offset exponential distribution of mean 478.6, the age of the oldest purported mussel *Dipleurodonta*, as derived from the PBDB.

Analyses were performed using the uniform tree prior using the independent gamma rates (IGR) clock model. A diffuse prior for the clock rate was established using a normal distribution with mean of 0.001 and standard deviation of 0.01 substitutions per site per million years. The  $mkv$  model was applied to the morphological partition with the molecular dataset analysed under the LG model, which was chosen as the best fit available amino acid model using ModelGenerator<sup>36</sup>. 20,000,000 generations were requested and convergence was assessed using Tracer v1.6. Analyses were considered converged when all parameters had ESS scores over 200, PSRF scores around 1.00 and the average deviation of split frequencies was below 0.01. Burn in was determined by graphically assessing the trace files.

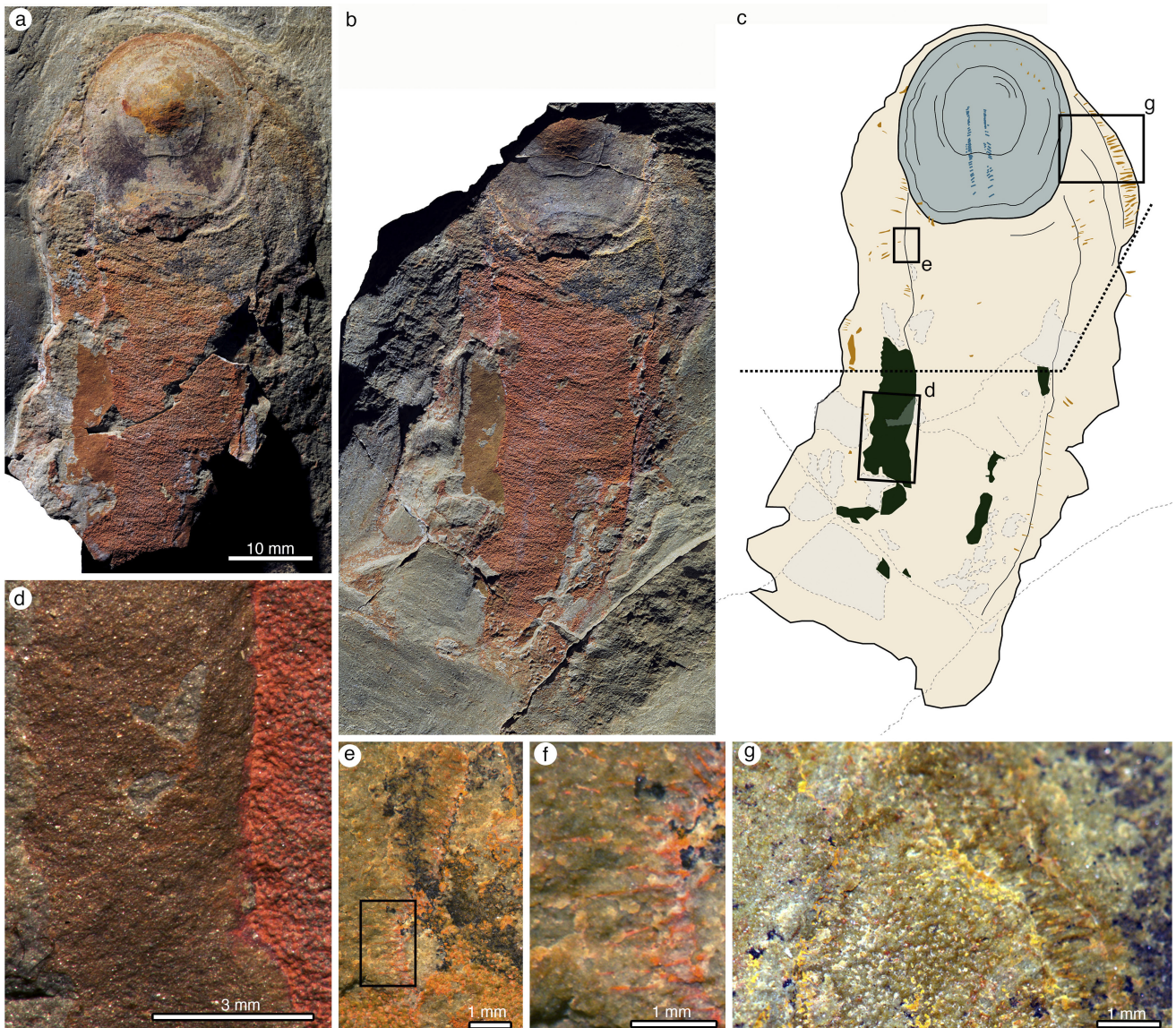
Two different total evidence analyses were performed. For the first analysis, the topology was left unconstrained. This analysis recovered a mean age for the molluscan crown of 556 Ma (549–562 Ma, 95% HPD), which is approximately 7 Ma older than the age of the oldest (non-molluscan) shelly fossils from the Nama group. A maximum age constraint of 549 Ma was therefore established for the molluscan crown group<sup>37</sup>. For the second analysis, this calibration was used, treating this age constraint as a maximum on the age of crown Mollusca using a uniform distribution. This resulted in improved resolution within total group Aculifera and a mean age for crown group molluscs of 543.4 Ma. Both analyses recovered sachtids as stem-group aculiferans.

**Data availability.** Nexus files, containing morphological and molecular sequences used in the phylogenetic analyses as well as the necessary commands to execute the total evidence analysis are provided in the Supplementary Data. Higher resolution versions of the figures can be obtained upon request from the corresponding author.

- Goloboff, P. A., Farris, J. S. & Nixon, K. C. TNT, a free program for phylogenetic analysis. *Cladistics* **24**, 774–786 (2008).
- Ronquist, F. *et al.* MrBayes 3.2: efficient Bayesian phylogenetic inference and model choice across a large model space. *Syst. Biol.* **61**, 539–542 (2012).
- O'Reilly, J. E. & Donoghue, P. C. Tips and nodes are complementary not competing approaches to the calibration of molecular clocks. *Biol. Lett.* **12**, 20150975 (2016).
- Boag, T. H., Darroch, S. A. & Laflamme, M. Ediacaran distributions in space and time: testing assemblage concepts of earliest macroscopic body fossils. *Paleobiology* **42**, 574–594 (2016).
- Waggoner, B. The ediacaran biotas in space and time. *Integr. Comp. Biol.* **43**, 104–113 (2003).
- Keane, T. M., Creevey, C. J., Pentony, M. M., Naughton, T. J. & McInerney, J. O. Assessment of methods for amino acid matrix selection and their use on empirical data shows that ad hoc assumptions for choice of matrix are not justified. *BMC Evol. Biol.* **6**, 29 (2006).
- Benton, M. J. *et al.* Constraints on the timescale of animal evolutionary history. *Palaeontol. Electronica* **18**, 1–106 (2015).

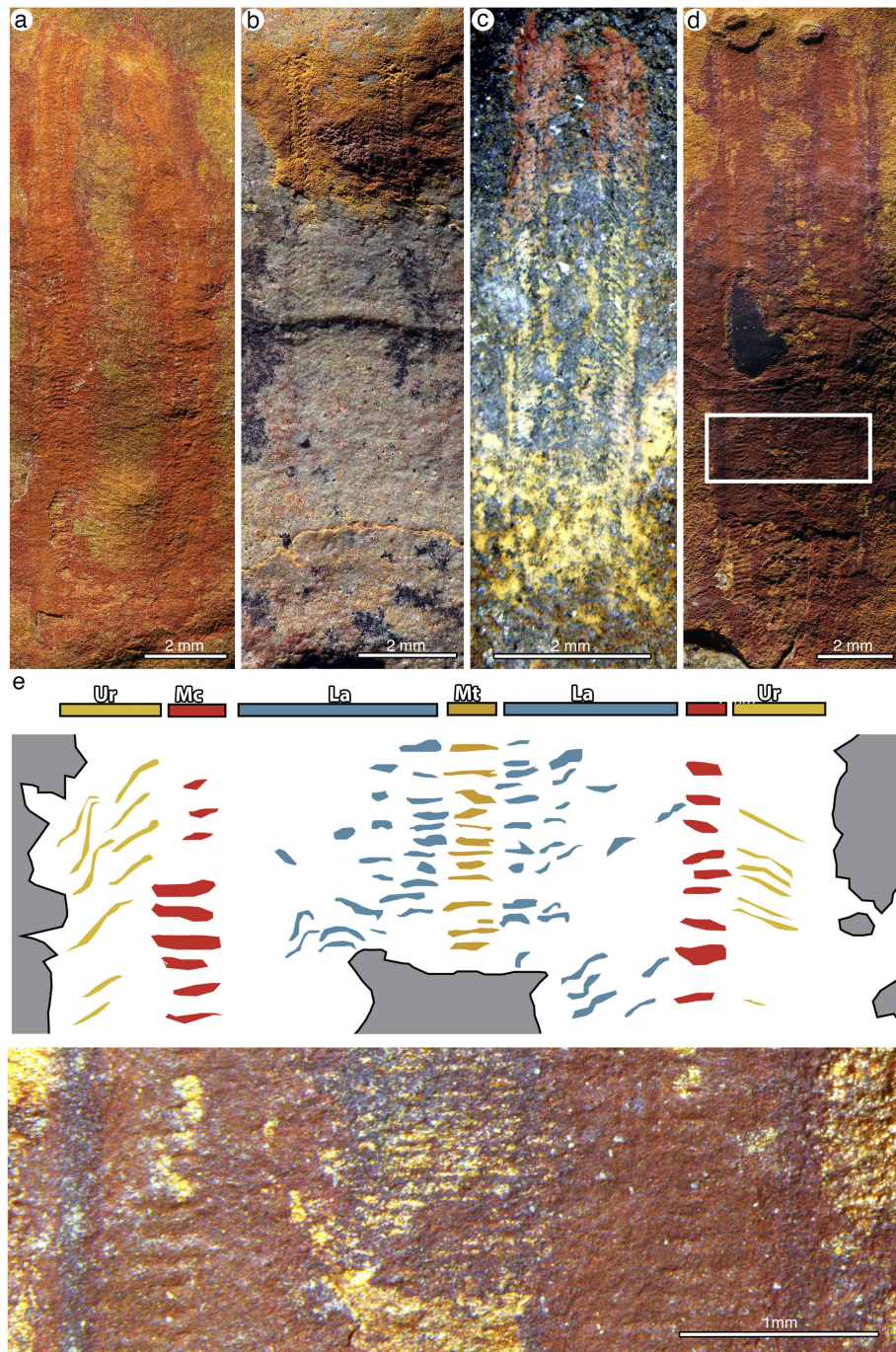


**Extended Data Figure 1** | *C. kroegeri* YPM 237255, holotype. **a**, Part, illuminated from the northwest. **b**, Counterpart, illuminated from the southwest and then mirrored horizontally. **c**, Part, submerged in water.

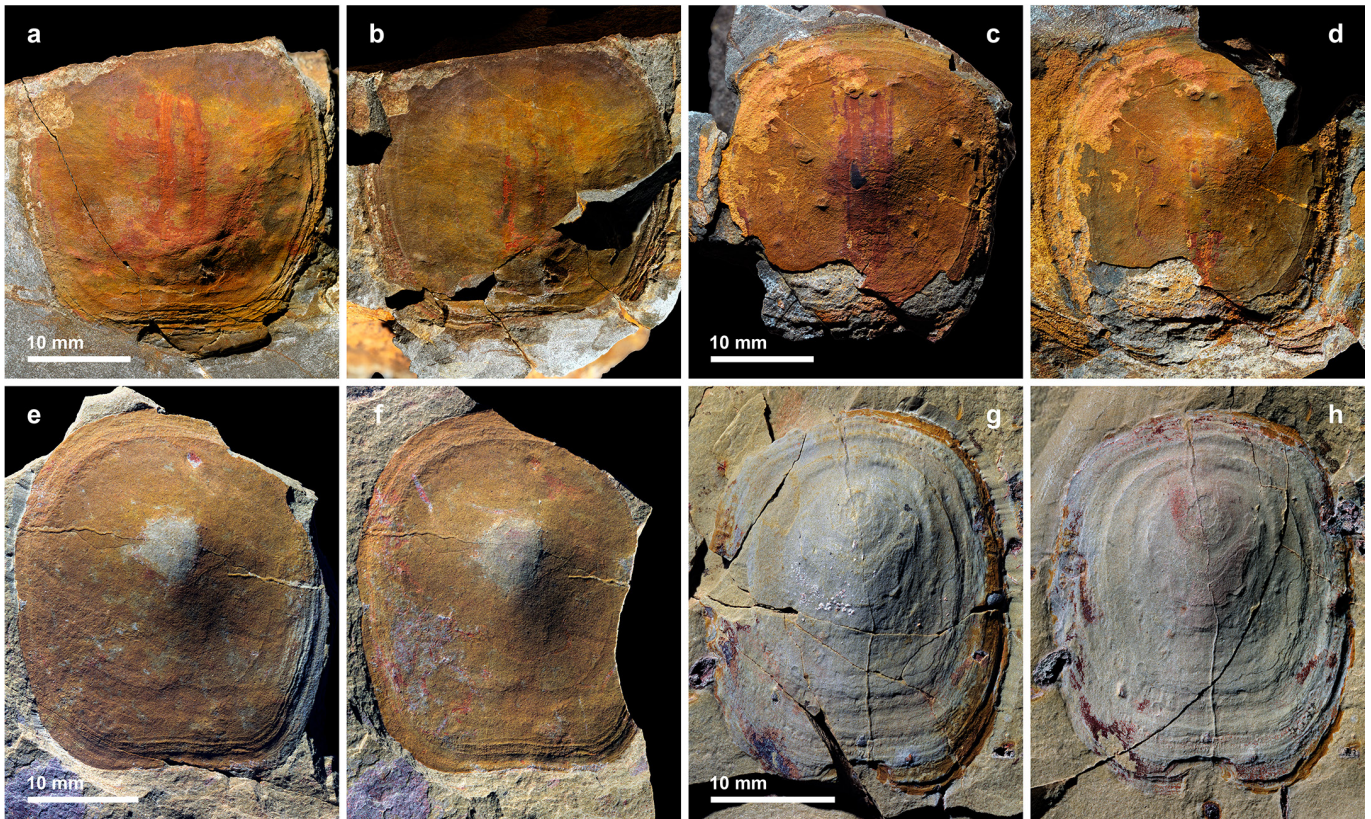


**Extended Data Figure 2 | *C. kroegeri* YPM 227515, paratype.** **a**, Part, illuminated from the northwest. **b**, Counterpart, illuminated from the southwest and then mirrored horizontally. **c**, Interpretative drawing of YPM 227515 with part and counterpart combined. Interpretations below the stippled line are derived from the counterpart. Boxes denote position of details shown in **d**, **e**, **g**. Areas shown in green are of the exposed ventral mantle, areas within dashed lines denote gaps in preservation, dark blue

shows the teeth of the radula and light blue denotes the shell. Sclerites are shown in orange but are only drawn where lying flat or covering the shell. **d**, Exposed ventral mantle, which is preserved in darker colouration but shows no visible sclerites. **e**, Folded dorsal mantle which preserves dorsal sclerites. **f**, Dorsal sclerites in longitudinal section. Boxed area is magnified in **f**. **f**, Dorsal sclerites. **g**, Dorsal sclerites in cross-section and marginal sclerites in longitudinal section.

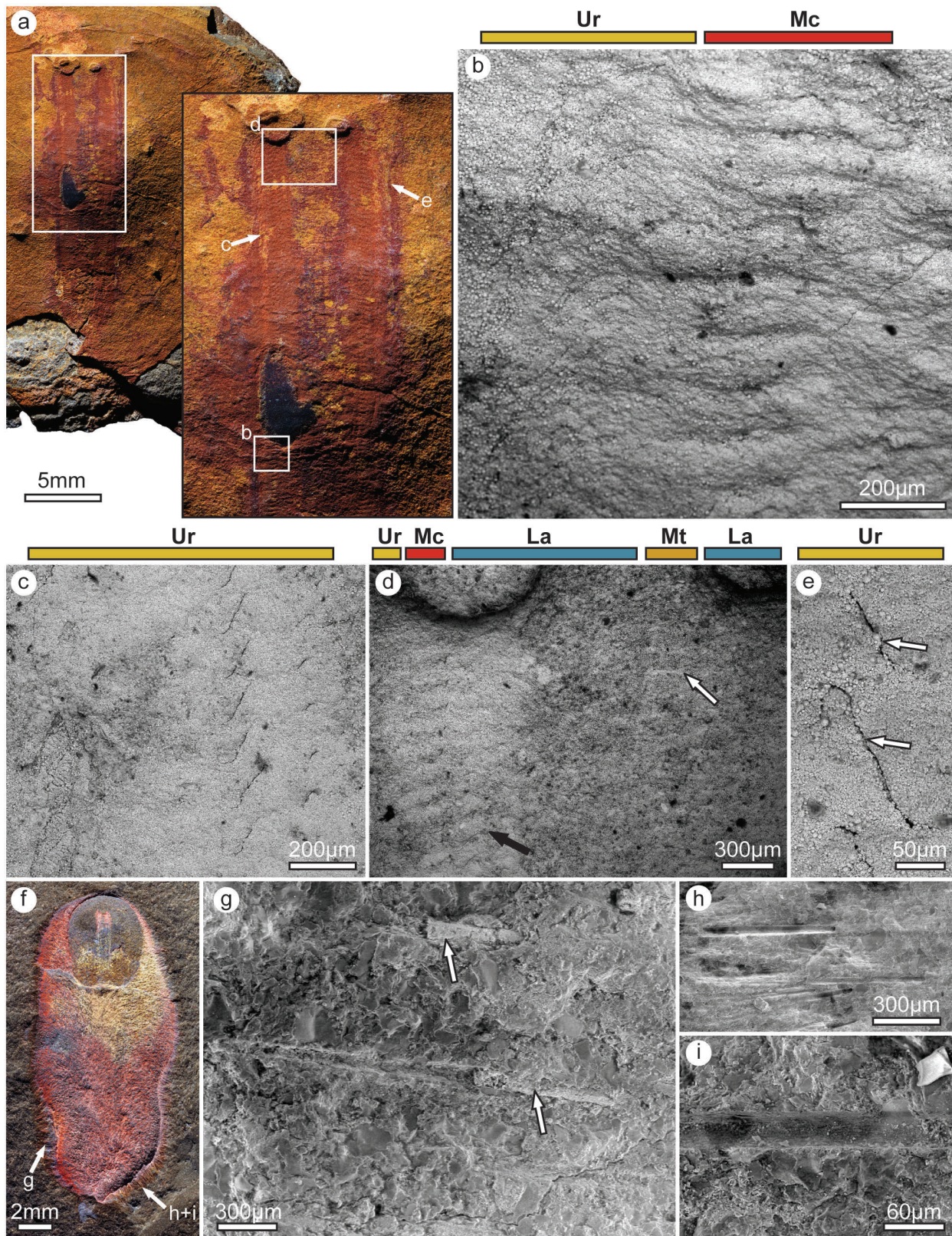


**Extended Data Figure 3 | The radula of *C. kroegeri*.** a, YPM 530837. b, YPM 227515. c, YPM 237255. d, YPM 530836. e, detail of d (bottom) with explanatory drawing (top) showing basal attachment points of radula teeth. Ur, uncinal region; Mc, major cusp; La, lateral area; Mt, median tooth. Dark grey areas areas obscured by overlying mineral.



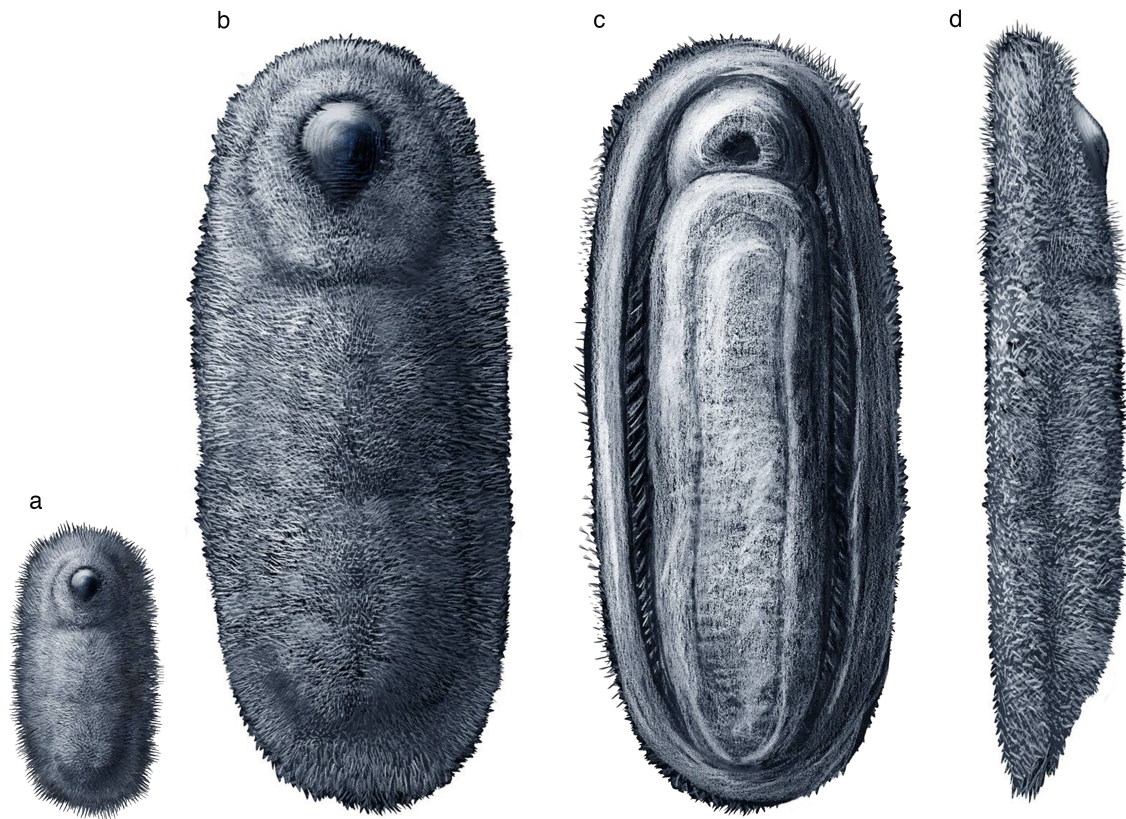
**Extended Data Figure 4 | Additional specimens of *C. kroegeri* and *Calvapilosa* sp. a.** **a**, Part of YPM 530837, isolated head valve with radula preserved. **b**, Counterpart of YPM 530837, mirrored. **c**, Part of YPM 530836, isolated head valve with radula preserved. **d**, Counterpart of

YPM 530836, mirrored. **e**, Part of YPM 530835, isolated head valve. **f**, Counterpart of YPM 530835, mirrored. **g**, Part of YPM 227641, *Calvapilosa ?kroegeri*, isolated head valve. **h**, Counterpart of YPM 227641, mirrored.

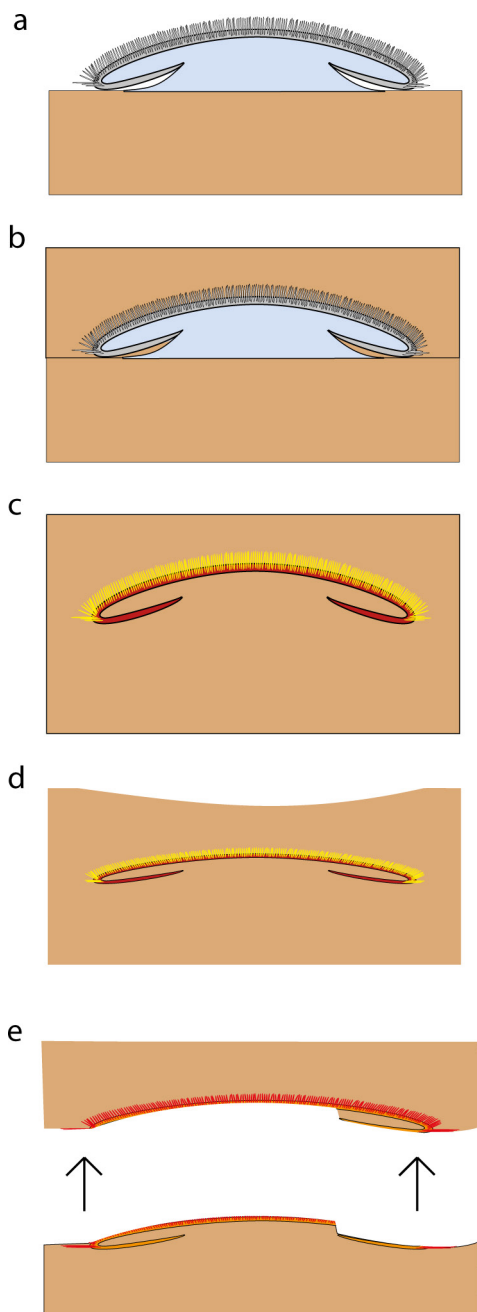


**Extended Data Figure 5 | SEM images of *C. kroegeri* sclerites and radula.** **a**, YPM 530836 indicating regions of photomicrographs **b–e**. **b**, Left major cusps and adjacent uncinial teeth. **c**, Left uncinial region. **d**, Overview showing median teeth (a single tooth indicated by the white arrow), broad flanking region with lateral teeth (a single tooth indicated

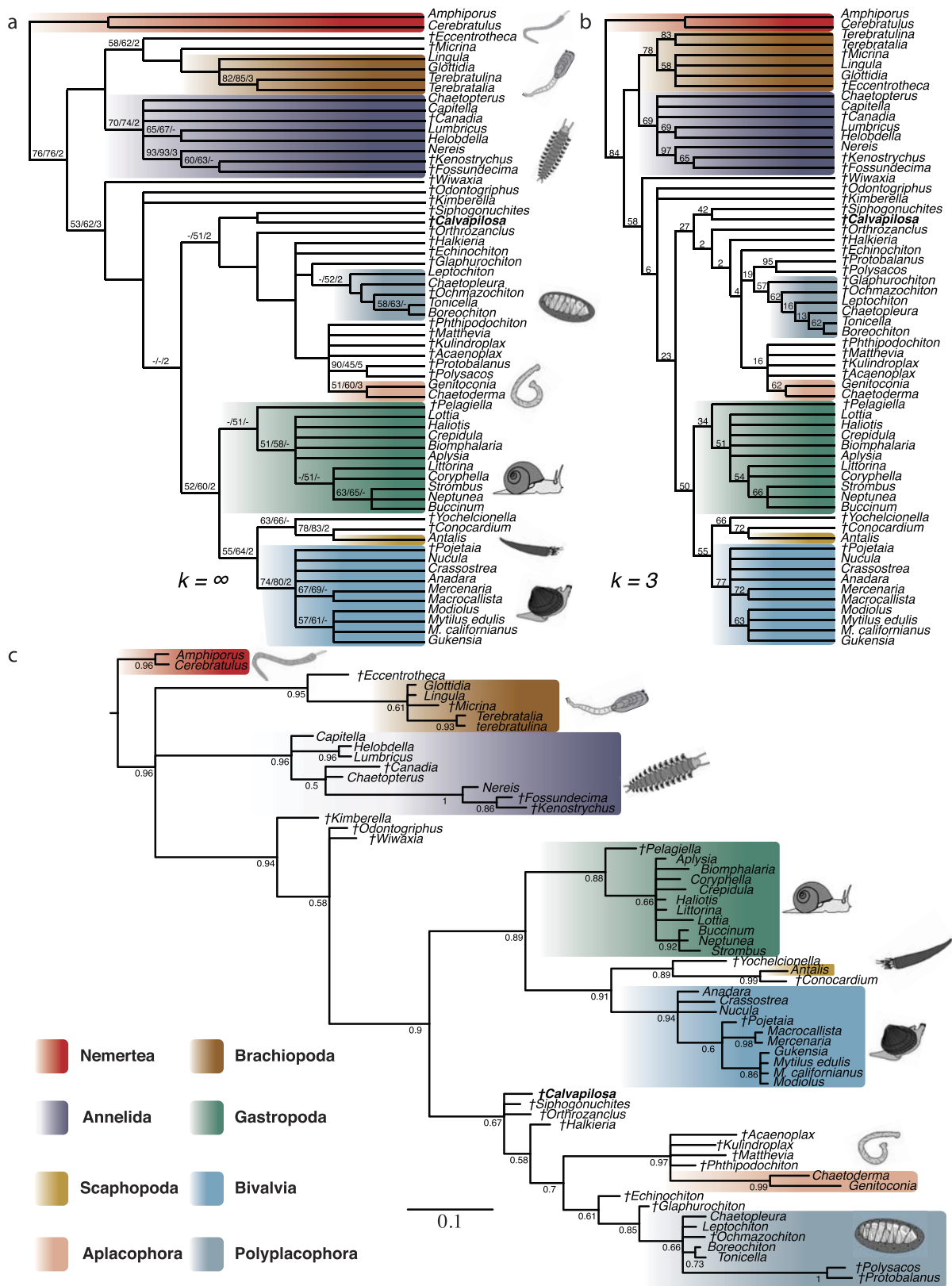
by the black arrow) and major cusps. **e**, Right uncinial teeth. **f**, YPM 237255 indicating regions of SEM photomicrographs **g–i**. **g**, Sclerites with diagenetic infill (white arrows). **h**, Sclerites in longitudinal section. **i**, Sclerite in longitudinal section preserved as a void. **b–h** and **g–i** were taken using backscatter and secondary electron imaging, respectively.



**Extended Data Figure 6 | Reconstruction of *C. kroegeri*.** a, Juvenile. b, Adult, dorsal view. c, Adult, lateral view. d, Adult ventral view. Drawing by Z. Dutta.

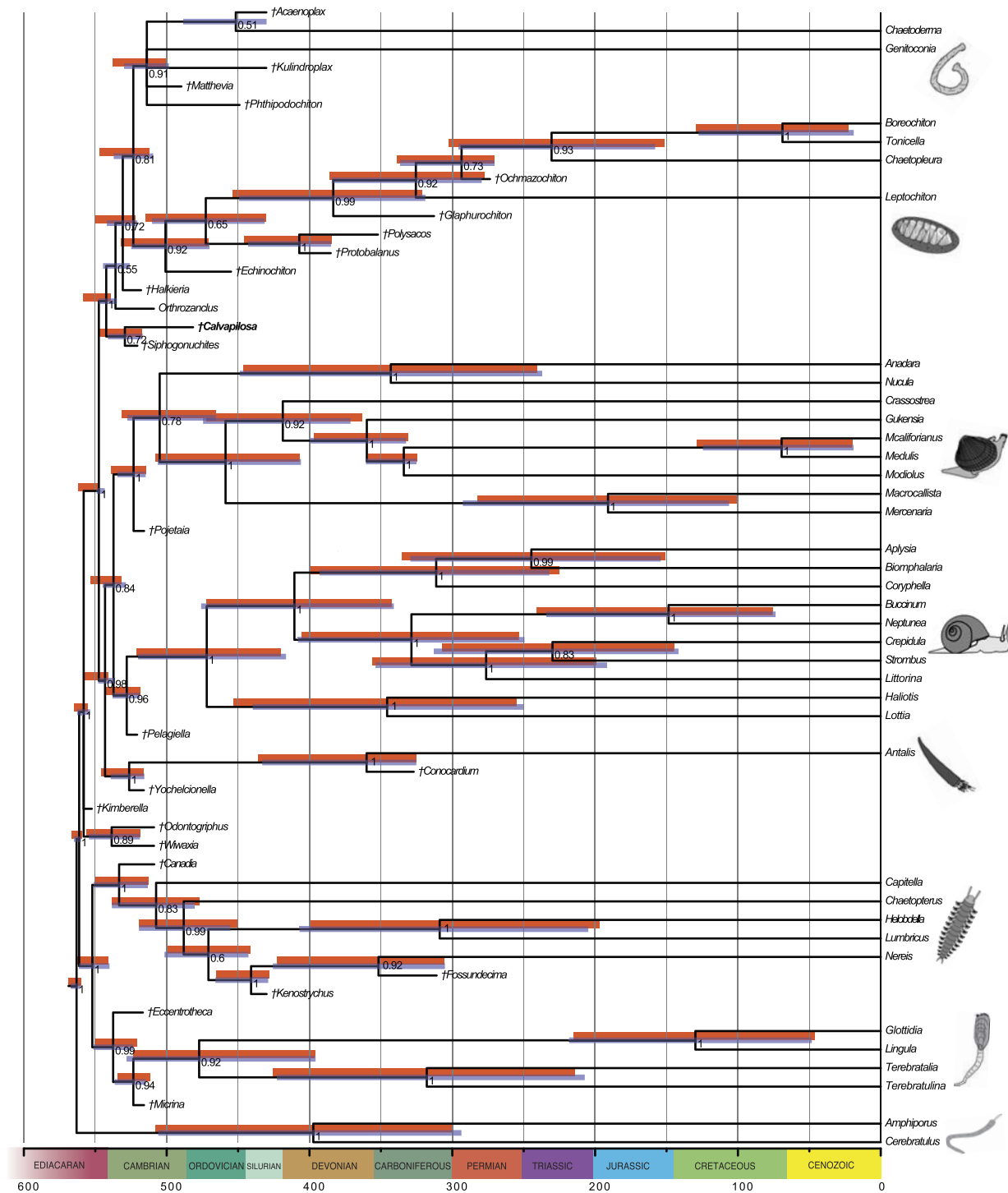


**Extended Data Figure 7 | Cartoon explaining preservation of YPM 227515, cross-sectional view. a, Prior to burial. b, Burial. c, Decay and replacement of the mantle and sclerites by pyrite. d, Compaction. e, Weathering and uneven splitting along the dorsal mantle, cross cutting sclerites and along smooth, ventral mantle.**



**Extended Data Figure 8 | Morphological phylogenetic analyses of molluscs incorporating *C. kroegeri*.** **a**, Strict consensus of 369 trees of length 209 steps from parsimony analysis under equal character weighting, numbers at the nodes are from 1,000 bootstrap replicates, 1,000 Jackknife

replicates and Bremer support, respectively. **b**, Parsimony analysis under implied weighting ( $k = 3$ ), numbers at the nodes are from 1,000 replicates of symmetric resampling. **c**, Results of Bayesian analysis using the  $mkv + \Gamma$  morphology model, numbers at the nodes are posterior probabilities.



**Extended Data Figure 9 | Bayesian total evidence dating analysis incorporating *C. kroegeri*.** Analysis performed using the uniform tree prior and  $LG + \Gamma$  and  $mkv + \Gamma$  for the molecular and morphological data, respectively. The topology shown is for analysis using a 549 Ma maximum

for the age of the molluscan crown group. Error bars on the node ages are 95% HPD intervals for both unconstrained analyses (red) and analyses with the maximum age constraint on molluscs (purple). Numbers at the nodes are posterior probabilities from the constrained analysis.